Cell

The ATAC Acetyltransferase Complex Coordinates MAP Kinases to Regulate JNK Target Genes

Tamaki Suganuma,[1] Arcady Mushegian,[1,2] Selene K. Swanson,[1,3] Susan M. Abmayr,[1,3] Laurence Florens,[1] Michael P. Washburn,[1,4] and Jerry L. Workman[1,*]
[1]Stowers Institute for Medical Research, 1000 East 50th Street, Kansas City, MO 64110, USA
[2]Department of Microbiology, Molecular Genetics, and Immunology
[3]Department of Anatomy and Cell Biology
[4]Department of Pathology and Laboratory Medicine
University of Kansas Medical Center, Kansas City, KS 66160, USA
*Correspondence: jlw@stowers.org
DOI 10.1016/j.cell.2010.07.045

SUMMARY

In response to extracellular cues, signal transduction activates downstream transcription factors like c-Jun to induce expression of target genes. We demonstrate that the ATAC (*A*da *t*wo *A* *c*ontaining) histone acetyltransferase (HAT) complex serves as a transcriptional cofactor for c-Jun at the Jun N-terminal kinase (JNK) target genes *Jra* and *chickadee*. ATAC subunits are required for c-Jun occupancy of these genes and for H4K16 acetylation at the *Jra* enhancer, promoter, and transcribed sequences. Under conditions of osmotic stress, ATAC colocalizes with c-Jun, recruits the upstream kinases Misshapen, MKK4, and JNK, and suppresses further activation of JNK. Relocalization of these MAPKs and suppression of JNK activation by ATAC are dependent on the CG10238 subunit of ATAC. Thus, ATAC governs the transcriptional response to MAP kinase signaling by serving as both a coactivator of transcription and as a suppressor of upstream signaling.

INTRODUCTION

Histone acetyltransferase complexes have been isolated from multiple organisms and shown to be involved in nuclear events that relate to chromatin biology (Kimura et al., 2005; Lee and Workman, 2007). The *Drosophila* ATAC (*A*da *t*wo *A* *c*ontaining) complex consists of 13 proteins and includes two distinct histone acetyltransferases, Gcn5/KAT2 and Atac2/KAT14 (Figure 1A). Whereas Gcn5/KAT2 preferentially acetylates histones H3K9 and H3K14, Atac2/KAT14 acetylates H4K16 (Ciurciu et al., 2006; Guelman et al., 2006; Suganuma et al., 2008). The Gcn5/KAT2, Ada3, and CG30390 (Sgf29 in yeast) subunits of ATAC are shared with SAGA (Spt-Ada-Gcn5 acetyltransferase) (Suganuma et al., 2008), an important transcriptional coactivator complex (Lee and Workman, 2007). However, it was unknown whether ATAC functions as a transcription cofactor like SAGA.

Mitogen-activated protein kinases (MAPKs) and their target kinases in the pathway lead to phosphorylation of target transcription factors (Edmunds and Mahadevan, 2004; Thomson et al., 1999). Exposure of cells to increases in extracellular osmolality results in rapid activation of stress-activated MAPKs (SAPKs), including c-Jun-NH_2-terminal kinase (JNK/basket in *Drosophila*) and p38 MAPKs (de Nadal et al., 2002; Edmunds and Mahadevan, 2004; Kyriakis and Avruch, 2001). Osmotic stress causes activation of JNK by phosphorylation which, in turn, phosphorylates c-Jun and enhances its transcriptional activity (Kayali et al., 2000; Thomson et al., 1999). MAPKs are more intimately involved in the regulation of downstream target genes than just phosphorylation of target transcription factors (Dioum et al., 2009). For example, the yeast SAPK Hog1 is recruited to target genes in chromatin and interacts with transcription factors, cofactors, and RNA polymerase II (Alepuz et al., 2001, 2003; de Nadal et al., 2004; Mas et al., 2009; Pokholok et al., 2006; Proft et al., 2006; Zapater et al., 2007). Recently, the ERK2 MAPK was found to bind with sequence specificity to DNA and act as a transcriptional repressor of interferon-γ-induced genes (Hu et al., 2009). Moreover, multiple MAPKs, including ERK1/2, p38, and JNK, bind to and regulate transcription of the *insulin* gene (Lawrence et al., 2009). Thus, MAPKs play important chromatin-associated functions in the regulation of gene expression.

MBIP (*M*APK upstream kinase [MUK] *b*inding *i*nhibitory *p*rotein), a component of the human ATAC complex, was identified as a MUK binding partner in a yeast two-hybrid screen (Fukuyama et al., 2000). The *Drosophila* ATAC component CG10238 encodes the *Drosophila* homolog of MoaE, a subunit of molybdopterin (MPT) synthase, an essential enzyme involved in the synthesis of the molybdenum cofactor (Moco). Moco binds molybdenum in the active site of molybdenum enzymes, which catalyze redox reactions as part of ancient and conserved biosynthetic pathways (Iyer et al., 2006; Leimkuhler et al., 2003; Rudolph et al., 2001; Schwarz and Mendel, 2006). However, CG10238 also contains C-terminal sequences that

A

		Purifications						
		CG10238	Atac2	CHRAC14	Ada2a	WDS	D12	Control
	Proteins	PEP (SC%)	PEP (SC%)	PEP (SC%)	PEP (SC%)	PEP (SC%)	PEP (SC%)	PEP (SC%)
ATAC	CG10238	29 (72.21)	5 (21.25)	2 (9.81)	7 (25.61)	6 (30.25)	16 (53.13)	0 (0)
	Gcn5/KAT	35 (46.69)	4 (6.15)	4 (6.4)	5 (8.24)	4 (7.38)	33 (33.95)	0 (0)
	Atac1	14 (53.37)	2 (5.34)	2 (7.58)	6 (16.3)	0 (0)	9 (20.71)	0 (0)
	Ada3	21 (58.89)	1 (1.98)	1 (1.98)	2 (7.19)	1 (3.24)	10 (16.37)	0 (0)
	Ada2a	20 (48.2)	2 (4.93)	2 (4.93)	9 (18.6)	0 (0)	18 (36.43)	0 (0)
	HCF	66 (68.87)	11 (11.93)	16 (17.6)	17 (19.87)	19 (18.07)	54 (49.4)	1 (2.6)
	D12	37 (45.86)	7 (9.08)	11 (19.81)	10 (13.62)	5 (9.7)	31 (38.29)	0 (0)
	CG30390	14 (56.60)	1 (5.88)	0 (0)	6 (26.64)	0 (0)	13 (55.36)	0 (0)
	Atac2/KAT14	26 (47.16)	10 (22.09)	7 (16.28)	5 (9.95)	5 (13.18)	19 (39.41)	0 (0)
	CHARC14	5 (62.5)	1 (10.16)	1 (10.16)	3 (27.34)	1 (14.84)	7 (71.88)	0 (0)
	Atac3	14 (40.88)	1 (3.89)	0 (0)	3 (7.61)	0 (0)	9 (20.71)	0 (0)
	NC2 beta	6 (60.66)	2 (14.21)	1 (7.1)	0 (0)	2 (14.21)	5 (27.32)	0 (0)
	WDS	18 (66.48)	7 (25.76)	5 (18.28)	8 (26.59)	20 (63.43)	13 (53.19)	1 (3.6)
Proteins related to JNK pathway	Jra	2 (10.03)	0 (0)	3 (19.03)	0 (0)	0 (0)	2 (13.84)	0 (0)
	Misshapen	16 (21.34)	0 (0)	5 (6.12)	0 (0)	0 (0)	5 (5.85)	0 (0)
	MKK4	4 (15.8)	0 (0)	0 (0)	0 (0)	0 (0)	0 (0)	0 (0)
	slik	5 (4.82)	0 (0)	0 (0)	0 (0)	0 (0)	0 (0)	0 (0)
	MEK3/MKK3	2 (8.08)	0 (0)	0 (0)	0 (0)	0 (0)	0 (0)	0 (0)
	Chickadee	2 (20.63)	0 (0)	0 (0)	0 (0)	0 (0)	0 (0)	0 (0)

B

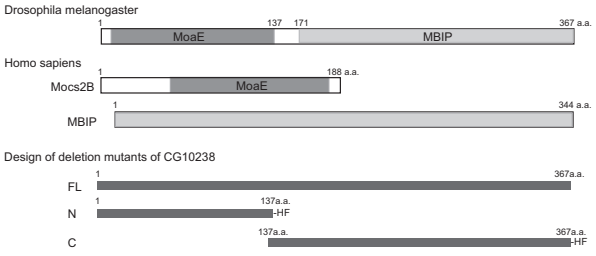

C

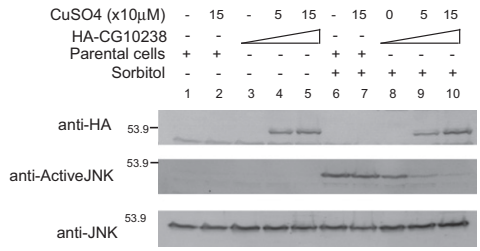

Figure 1. Peptides from Proteins Related to the JNK Pathway Were Detected in Purifications of ATAC Subunits, and CG10238 Inhibits JNK Activation by Osmotic Stress in *Drosophila* Schneider's S2 Cells

(A) Peptides of MAPK pathway proteins in addition to ATAC subunits detected by MudPIT analysis for affinity purifications of ATAC subunits with FLAG-HA-tagged CG10238, Atac2/KAT14, Ada2a, CHRAC14, WDS, and D12. Parental S2 cells were used in mock purification as a control. PEP, peptide count; SC%, sequence coverage (%).

(B) Homology domains of CG10238 and experimental design of truncation mutants. The diagram shows the domains of CG10238 that are homologous to human MOCS2B (hMoaE) and to human MBIP, which are separate proteins. The full-length (FL), N-terminal that contains only MoaE domain (N), and C-terminal that contains only MBIP protein sequences (C) were stably expressed in S2 cells (Figure 2; see Figure S1B).

(C) CG10238 inhibited the activation of JNK stimulated by osmotic stress in S2 cells. Stably expressed FLAG-HA-tagged CG10238 was induced by 0, 50, or 150 μM $CuSO_4$ in S2 cells. Cells were stimulated with osmotic stress by addition of 500 mM sorbitol for 12 min before harvesting cells (C, lanes 6–10; Figure 2C, lanes 5–14; Figure 2D, lanes 1–12; see Figures S2A–S2C). The nuclear extracts were examined by western blot probing with anti-HA, anti-Active JNK, and anti-JNK (C; Figure 2C). Parental S2 cells of stable cell lines cultured with 0 or 150 μM $CuSO_4$ were used as controls (C, lanes 1, 2, 6, and 7; see Figure S3). See also Figures S1, S2, and S3.

are homologous to human MBIP. This observation, coupled with the presence of MAPK signaling proteins in ATAC purifications, led us to ask whether CG10238 and ATAC play a role in MAPK signaling.

RESULTS

ATAC Interacts with Proteins Related to the MAPK Pathway

Affinity purifications of the ATAC complex revealed proteins that are part of the MAPK signaling pathway (Figure 1A; see Figure S1A available online). Peptides from these proteins were found in purifications via the CG10238, CHRAC14, and D12 ATAC subunits. Peptides were identified from the transcription factor Jra (*J*un-*r*elated *a*ntigen), the *Drosophila* homolog of c-Jun, and Misshapen (MSN), the *Drosophila* homolog of Ste-20 kinase (Figure 1A) (Morrison et al., 2000; Su et al., 1998; Treisman et al., 1997). We also found peptides from other STE kinases, such as MKK4, slik, and MEK3/MKK3, as well as peptides from Chickadee, which has been shown to interact genetically with the JNK pathway (Jasper et al., 2001; Morrison et al., 2000).

The ATAC Subunit CG10238 Functions as an Inhibitor of JNK Activation in Response to Osmotic Stress

We tested whether CG10238 plays a role in MAPK signaling like MBIP (Fukuyama et al., 2000). MAPK cascades can be activated by osmotic stress, resulting in activation of JNK by phosphorylation (Kayali et al., 2000; Yang et al., 2003). We therefore examined whether expression of CG10238 affected the activation of JNK under conditions of osmotic stress (Kayali et al., 2000).

We first titrated the cellular response to osmotic stress stimulated by sorbitol in S2 cells by western blot (Figures S2A and S2B). Maximum activation of JNK was observed between 7 and 30 min after treatment with a minimum concentration of 500 mM sorbitol (Figure S2A, lane 5; Figure S2B, lanes 2–4). We then examined the level of JNK activation in cells expressing CG10238 in the presence or absence of osmotic stress induced by 500 mM sorbitol for 12 min. Expression of CG10238 was inducible by $CuSO_4$, and parental S2 cells were treated with

A

CG10238-Domain	N	C
ATAC subunits	PEP(SC%)	PEP(SC%)
CG10238-PA	7 (25.6)	17 (50.95)
Gcn5/KAT	0 (0)	8 (12.67)
Atac1	0 (0)	3 (9.55)
Ada3	0 (0)	3 (8.99)
Ada2a	0 (0)	5 (13.09)
HCF	5 (1.47)	24 (26.8)
D12	0 (0)	15 (21.26)
CG30390	0 (0)	3 (13.15)
Atac2/KAT14	0 (0)	5 (10.98)
CHRAC14	0 (0)	0 (0)
Atac3	0 (0)	2 (6.55)
NC2beta	0 (0)	3 (14.21)
WDS	1 (3.88)	6 (27.42)

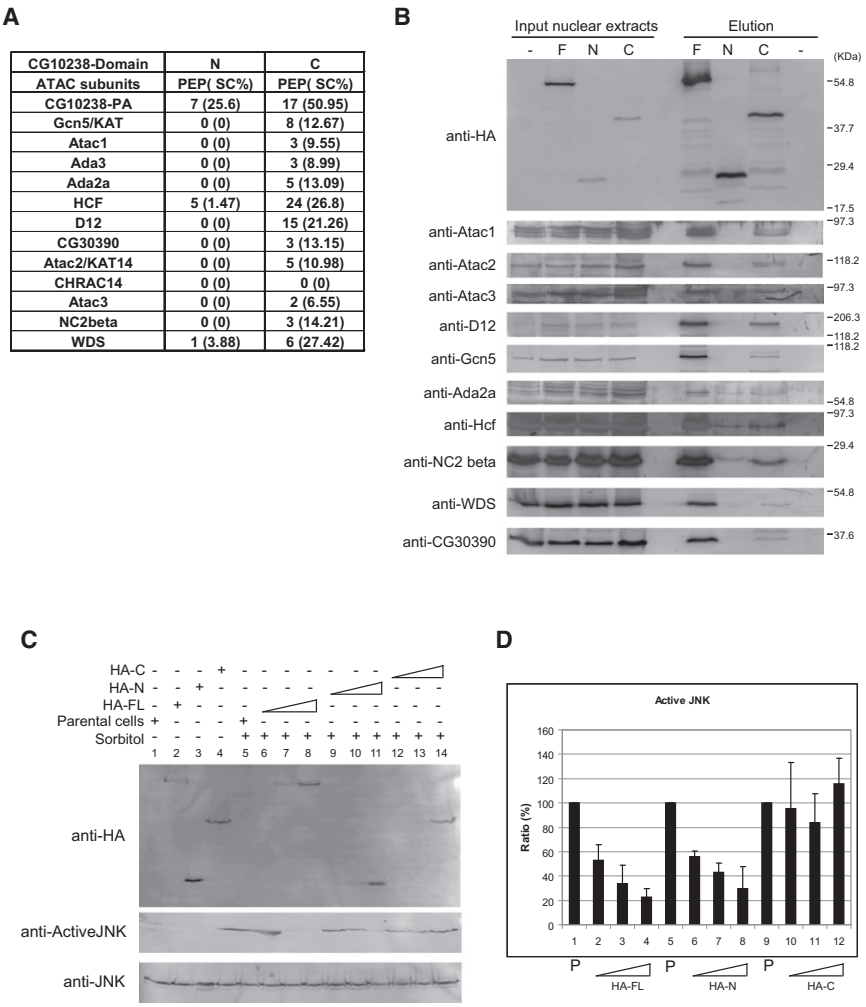

Figure 2. MBIP-Related Sequences Incorporate CG10238 into ATAC; However, the MoaE Domain Inhibits JNK Activation

(A) FLAG-HA-tagged N terminus that contains only the MoaE domain (N) and C terminus that contains only MBIP protein sequences (C) were stably expressed in S2 cells purified by FLAG affinity beads. The copurified proteins were examined by MudPIT analysis (see Figures S1A and S1B). The observed PEP and SC (%) of each sample are indicated as in Figure 1.

(B) The copurified proteins of CG10238-full-length (F), -N, or -C (Figure 1B; Figure S1) were analyzed by western blotting with antibodies against HA tag and ATAC subunits. As a control, untransfected parental S2 cells were mock purified and analyzed by western blotting (-).

(C and D) The MoaE domain inhibits JNK activation. The ability to inhibit JNK activation was compared between FLAG-HA-tagged CG10238 (FL), CG10238-N (MoaE domain), and CG10238-C (MBIP domain) after the expression levels were normalized (see also Figure S1B). Parental S2 cells cultured with 150 μM $CuSO_4$ were used as a positive control (C, lanes 1 and 5; D, lanes 1, 5, and 9). Osmotic stress was induced as in Figure 1C (see also Figures S2A and S2B). For sorbitol-stimulated samples, the intensity of each band for Active JNK in western blotting was quantified, and each sample from CG10238 (FL), CG10238-N, and CG10238-C was individually compared with the intensity of parental cells (P), and the ratios (%) are shown in (D). The average of four independent experiments is graphed. Error bars represent standard deviation.

See also Figures S1 and S2.

the same amount of $CuSO_4$ and sorbitol as controls. We first confirmed by western blot that the expression level of HA-tagged CG10238 in the stable cell line without induction was similar to that of endogenous CG10238 in the parental cells (Figure S2C). Active JNK was not detected in the absence of sorbitol treatment, or upon induction of CG10238 by addition of $CuSO_4$ (Figure 1C, lanes 1 and 2). In the presence of sorbitol, JNK was activated in the parental cells (Figure 1C, lanes 6 and 7). However, induction of CG10238 expression by $CuSO_4$ inhibited the activation of JNK in a dose-dependent manner (Figure 1C, lanes 8–10). Thus, CG10238 inhibits JNK activation by osmotic stress in vivo. Because JNK is also activated by ultraviolet light (UV), we examined whether the inhibitory activity of CG10238 extended to this JNK activation mechanism (Angel et al., 1988; Devary et al., 1991; Rozek and Pfeifer, 1995). Expression of CG10238 also inhibited activation of JNK by UV (Figure S3).

The MBIP Domain of CG10238 Is Required for Incorporation into the ATAC Complex

The finding that CG10238 prevented JNK activation when expressed in vivo led us to ask whether CG10238 served this function in isolation or as part of the ATAC complex. We first examined the two parts of CG10238 to determine which might incorporate it into the ATAC complex. We generated S2 cell lines that stably expressed tagged truncated forms of CG10238 that included only the N-terminal MoaE domain or the C-terminal MBIP domain (Figure 1B). These tagged proteins were affinity purified from the stable cell lines after their expression levels were normalized (Figure S1B). Proteins that copurified with each domain of CG10238 were identified by multidimensional protein identification technology (MudPIT) analysis and confirmed by western blots (Figures 2A and 2B; Figure S1A). All ATAC subunits except CHRAC14 associated with the MBIP domain. A few peptides from two of the ATAC subunits were detected by purification with the MoaE domain and three subunits were detected weakly by westerns (Figure 2B). Thus, the MBIP domain of CG10238 is responsible for incorporating the protein into the ATAC complex.

The MoaE Domain of CG10238 Inhibits JNK Activation

Analysis of the domain structure of MoaE and MBIP orthologs in a variety of organisms indicates that many insects encode these two domains as a translational fusion like that of *Drosophila* CG10238. By contrast, orthologs in nematodes, plants, fungi,

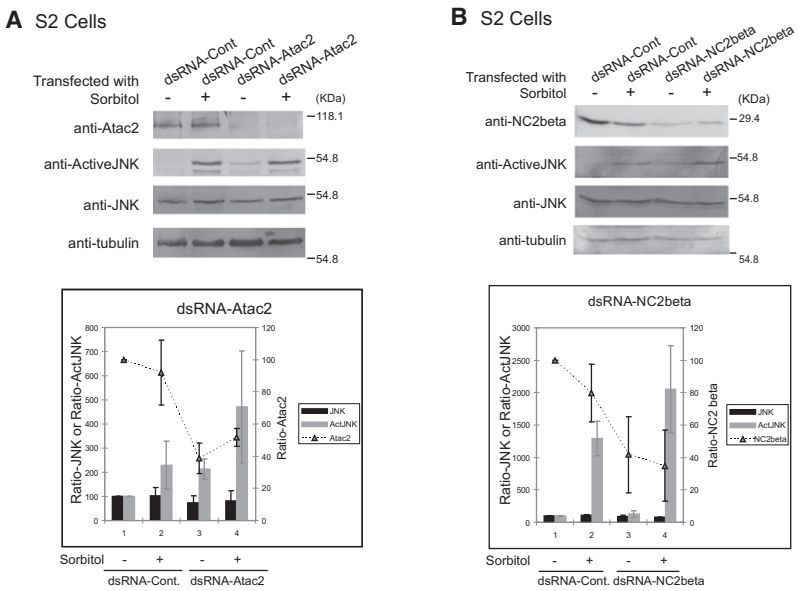

Figure 3. ATAC Inhibits JNK Signaling

S2 cells were transfected with dsRNA-Atac2, dsRNA-NC2 β, or dsRNA-Control (dsRNA-Cont) (A and B) (see Figure S4). 293T cells were transfected with dsRNA-hAtac2/CSRP2BP, dsRNA-MBIP, or dsRNA-Control (dsRNA-Cont) (C and D). The knockdown cells were then stimulated with or without 500 mM (for S2 cells) or 400 mM (for 293T cells) sorbitol as in Figure 1C (see Figure S2D). The nuclear extracts were examined by western blot probing with anti-Active JNK, anti-JNK, anti-Atac2 (A and C), anti-NC2 β (B), anti-MBIP (D), or anti-tubulin antibodies as a loading control (A–D, top). The intensities of each band of JNK, Active JNK, Atac2, NC2 β, hAtac2, or MBIP in western blotting were quantified from four independent experiments and plotted as ratios to the untreated control cells (A–D, bottom). Dark bars show the ratio of JNK intensities, light bars show the ratio of Active JNK intensities, and the dotted line shows the ratio of Atac2 (A), NC2 β (B), Atac2/CSRP2BP (C), or MBIP (D) intensities. Error bars represent standard deviation.
See also Figures S2 and S4.

and all prokaryotes except parasitic bacteria have a MoaE homology domain but are missing the MBIP domain. Sequence database searches using the PSI-BLAST program (Altschul et al., 1997) with human MBIP (GenBank accession number 119586267) as query revealed sequence matches between the N-terminal portion of MBIP orthologs from Metazoa and MoaE proteins. Thus, the N-terminal sequences of mammalian MBIPs are related to the MoaE sequences. Hence, our bioinformatic analysis suggests the N-terminal sequences of MBIP evolved from MoaE and raises the possibility that the MoaE domain of CG10238 contributes to the JNK inhibition activity.

We generated S2 cell lines that stably expressed tagged truncated forms containing the MoaE domain (N-terminal) or MBIP domain (C-terminal) (Figure S1B), and then compared the inhibitory activities of the full-length protein to that of the MoaE and MBIP domains (Figures 2C and 2D). Full-length CG10238 and the MoaE domain alone inhibited activation of JNK (Figure 2C, lanes 6–11; Figure 2D, bars 1–8). However, the MBIP domain of CG10238 failed to prevent the activation of JNK (Figure 2C, lanes 12–14; Figure 2D, bars 9–12). Thus, the active portion of CG10238 in inhibition of JNK activation is the MoaE domain, whereas the C-terminal sequences connect this activity to the ATAC complex.

ATAC Inhibits JNK Activation

The MoaE domain of CG10238 was sufficient to prevent JNK activation when expressed in vivo, whereas the MBIP domain was required to incorporate CG10238 into ATAC (Figures 2A–2D). These data raised the question of whether ATAC itself plays a role in inhibition of the JNK pathway. To address this question, we examined JNK activation in S2 cells where endogenous subunits of ATAC were knocked down by dsRNA interference. The expression level of Atac2 was reduced 60% in cells expressing dsRNA-Atac2 (Figure 3A). Interestingly, JNK was partially activated upon reduction of Atac2 even in the absence of osmotic stress (Figure 3A). Moreover, activation of JNK by osmotic stress was enhanced in the Atac2 knockdown cells (Figure 3A). We observed similar results upon knockdown of NC2 β or CG10238 subunits of ATAC by dsRNA (Figure 3B; Figure S4A). Although JNK activation was not observed in D12 knockdown cells without osmotic stress, its activation was also increased in these cells under conditions of osmotic stress (Figure S4B). Because human MBIP was recently shown to be a component of the human ATAC complex (Fukuyama et al., 2000; Wang et al., 2008), it was of interest to determine whether human ATAC inhibited the activation of JNK by osmotic stress in human

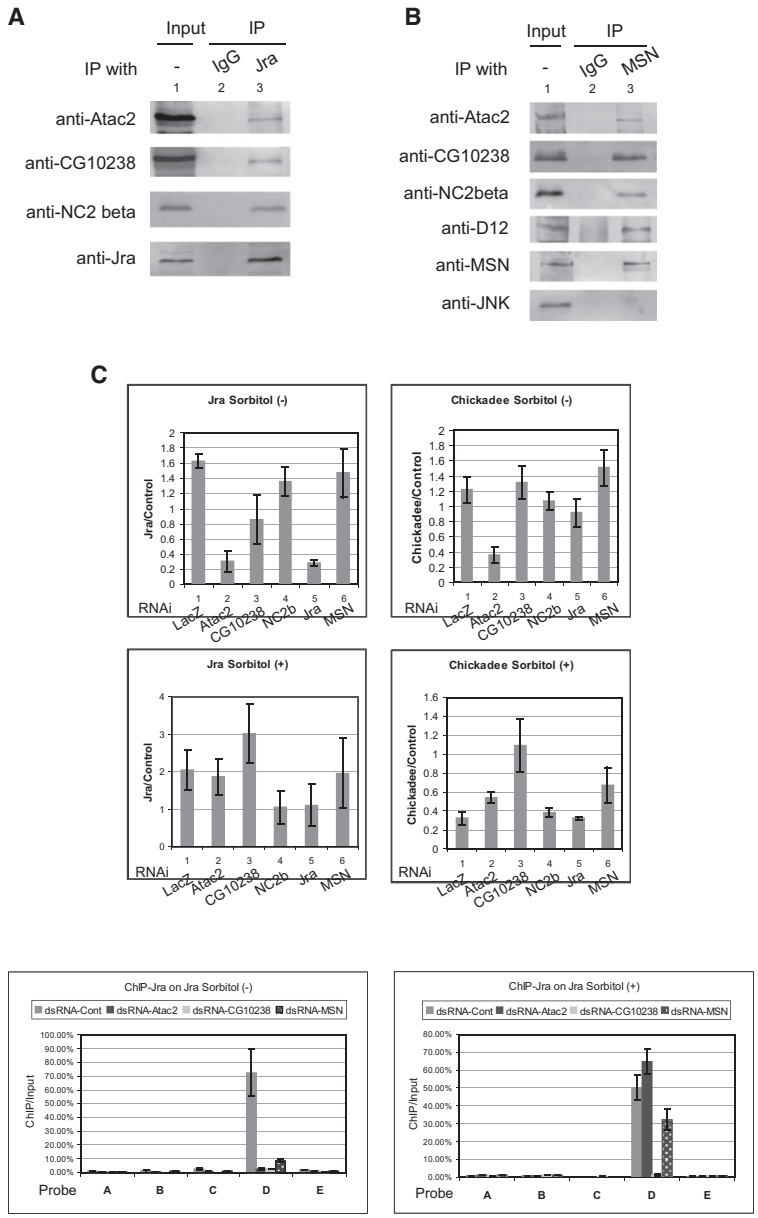

Figure 4. ATAC Is Required for the Transcription Regulation of JNK Target Genes

(A and B) Extracts from S2 cells endogenously expressing ATAC subunits and JNK (B) were immunoprecipitated with antibodies to endogenous Jra (A) or Misshapen (MSN) (B). The presence of ATAC subunits, MSN, and JNK in the input and immunoprecipitates (IP) was detected by western blots.

(C) Quantitative real-time RT-PCR (qRT-PCR) of Jra and Chickadee mRNA in S2 cells transfected with dsRNA-LacZ (Control), dsRNA-Atac2, dsRNA-CG10238, dsRNA-NC2 β (NC2b), dsRNA-Jra, or dsRNA-MSN (see Figure S5A). Gene-specific mRNA levels from the cells without sorbitol stimulation (C, top) and 30 min after 500 mM sorbitol stimulation (C, bottom) were measured and normalized to RpL-32 expression (Figure S5B), and are represented as ratios by qRT-PCR measurements. The average of three independent experiments is graphed. Error bars represent standard deviation.

(D) ChIP assays were performed with an antibody against Jra from S2 cells without sorbitol stimulation (D, left) or with sorbitol stimulation (D, right) expressing dsRNA-LacZ (Cont), dsRNA-Atac2, dsRNA-CG10238, or dsRNA-MSN (D) (Figures 5B–5M). The association of Jra on the probed region of the *Jra* gene as indicated in Figure 5A, and input chromatin was measured by qRT-PCR and normalized to input, and the ratios of quantities are represented (see Figure S6). The average of three independent experiments is graphed. Error bars represent standard deviation.

See also Figures S2, S5, and S6.

293T cells (Figure S2D). Indeed, JNK was activated to higher levels upon knockdown of MBIP or CSRP2BP (human homolog of Atac2) in 293T cells (Figures 3C and 3D). These data indicate that the ATAC complex is required for complete inhibition of JNK activation in both *Drosophila* and human cells.

ATAC Functions as Transcriptional Cofactor for JNK Target Genes

The presence of peptides from the Jra transcription factor in MudPIT analyses of the affinity-purified ATAC complex (Figure 1A) suggests that ATAC interacts with Jra and may serve as a transcriptional cofactor. Indeed, endogenous Jra was able to coimmunoprecipitate with Atac2, CG10238, and NC2 β, subunits of ATAC (Figure 4A). We also sought to confirm the interaction of MSN (Figure 1A), the *Drosophila* Ste-20 kinase, with ATAC in vivo. Endogenous Atac2, CG10238, NC2 β, and D12 coimmunoprecipitated with endogenous MSN (Figure 4B).

If ATAC serves as a cofactor for Jra, then Jra-dependent transcription would require ATAC and ATAC should be localized to Jra target genes. Because the gene encoding c-Jun, the mammalian homolog of Jra, is positively regulated by c-Jun protein (Angel et al., 1988), we examined whether ATAC functions in *Jra* transcription. We measured the levels of *Jra* transcripts by quantitative real-time RT-PCR (qRT-PCR) of control and ATAC knockdown S2 cells. As a control, we confirmed that *Jra* transcript levels were reduced in cells expressing dsRNA-Jra compared with cells expressing control-dsRNA-LacZ (Figure 4C, upper left). Importantly, *Jra* transcript levels were significantly reduced in Atac2 and CG10238 knockdown cells and slightly reduced in NC2 β knockdown cells (Figure 4C, upper left). We did not detect effects on *Jra* transcripts in MSN knockdown cells. We confirmed that the transcripts of *atac2*, CG10238, *nc2* β, and *msn* were reduced by expression of each dsRNA-Atac2, dsRNA-CG10238, dsRNA-NC2 β, and dsRNA-MSN by qRT-PCR (Figure S5A). We also observed that the expression of Atac2 was increased in Jra knockdown (see below).

We next examined *chickadee*, another Jra target gene (Jasper et al., 2001). Transcript levels of *chickadee* decreased significantly upon knockdown of Atac2 and somewhat more modestly upon knockdown of NC2 β or Jra (Figure 4C).

Transcript levels of *chickadee* were not reduced significantly in CG10238 knockdown cells. Of note, we did not observe changes in the transcript levels of target genes of a different H4K16 acetyltransferase complex (MSL) upon knockdown of ATAC, indicating that requirement for ATAC is specific for *Jra* and *chickadee* (Figure S5B).

The JNK cascade is activated by osmotic stress and increases c-Jun expression in mammals. Thus, we examined *Jra* and *chickadee* transcript levels in ATAC knockdown cells upon treatment with sorbitol. Interestingly, *Jra* transcripts were not reduced in Atac2 knockdown cells upon osmotic stress but were increased in CG10238 knockdown cells. The expression of Chickadee was also increased in ATAC and MSN knockdown cells under osmotic stress. Thus, ATAC positively impacts the expression of JNK target genes in the absence of osmotic stress but plays a predominantly negative role at JNK target genes under conditions of osmotic stress. Moreover, the positive effects of ATAC on expression of JNK target genes are mediated primarily by Atac2, whereas its negative effects are most strongly dependent on CG10238.

ATAC Functions as a Cofactor for the JNK Target Gene *Jra*, and Coordinates Upstream MAPKs onto *Jra*

Previous studies have shown the direct association of MAPKs with gene loci that they regulate (de Nadal and Posas, 2010; Dioum et al., 2009). Thus, we measured the occupancy of ATAC and upstream kinases directly on JNK target genes. We examined the occupancy of ATAC on the *Jra* gene in ATAC and MSN knockdown cells by chromatin immunoprecipitation (ChIP) assay. Previous studies have shown that Jun can form a homodimer or heterodimerize with ATF or Fos to form the AP-1 transcription factor. The *c-Jun* promoter contains AP-1-like sequences (TTACCTCA and TGACATCA) in addition to an NF-jun binding sequence (GGAGTCTCC) (Rozek and Pfeifer, 1993). c-Jun was found to occupy the *c-Jun* promoter without external stimulus (Angel and Karin, 1991). We confirmed that Jra actually bound to the *Jra* gene by ChIP assay (Figure 4D, left). Jra was found to significantly occupy a site in the middle of the coding region that contains an NF-jun recognition sequence (Figure 4D, left). We analyzed regions of the *Jra* gene that are comparable to the regulatory regions of the human *c-Jun* gene (Figure 5A). We probed ATAC occupancy, with and without osmotic stress, at an upstream enhancer (primer A), the promoter containing the AP-1 binding sequence (primer B), the 5′ region of the coding sequence (primer C), the middle of the coding sequence that contained an NF-jun binding sequence (GGAGGCACC) (primer D), and a region 3′ of the coding sequence (primer E) (FlyBase and UCSC Genome Browser) (Figure 5A) (Rozek and Pfeifer, 1993).

In the absence of osmotic stress, Atac2 was found to occupy the enhancer and promoter regions of *Jra* (Figure 5B, dsRNA-Cont). As expected, Atac2 occupancy of these regions was reduced in the Atac2 knockdown cells (Figure 5B). Atac2 occupancy of the promoter was reduced in CG10238 but not MSN knockdown cells. As controls for the specificity of ATAC occupancy of *Jra*, we performed an ATAC-ChIP assay on two target genes of the MSL complex (Figures S5 and S6). Background signals on these genes were not affected by the knockdown of Atac2 or CG10238. We next investigated whether ATAC occupancy affected acetylation of the nucleosome on the *Jra* gene by a ChIP assay for H4K16 acetylation. In control cells without osmotic stress, both the enhancer and promoter regions were enriched in H4K16 acetylation, which was significantly reduced in the Atac2 and CG10238 knockdown cells (Figure 5D). Thus, in the absence of osmotic stress, ATAC occupied the enhancer and promoter of *Jra*, and H4K16 acetylation at these sites was dependent on ATAC.

In the presence of osmotic stress, ATAC occupancy and H4K16 acetylation of the promoter were similar but were reduced at the upstream enhancer (Figures 5C and 5E). Interestingly, ATAC occupancy and H4K16 acetylation of the coding region at primer D were stimulated by osmotic stress (Figures 5C and 5E). Jra was clearly localized on this region with or without osmotic stress (Figure 4D). Jra occupancy at primer D was strongly reduced in Atac2, CG10238, and MSN knockdown cells in the absence of sorbitol. However, under osmotic stress, Jra occupancy required primarily CG10238 (Figure 4D). Thus, under conditions of osmotic stress, ATAC occupancy at the upstream enhancer was reduced and instead increased in the coding region where Jra was bound.

We next tested whether stress-activated upstream kinases were recruited to the *Jra* gene. We probed Active JNK (phospho-JNK) and phospho-MKK4/SEK1 (Ser257/Thr261) occupancy on the *Jra* gene. We also tested for the occupancy of the MSN kinase. In the absence of osmotic stress in control cells, each of these kinases could be found on the *Jra* gene although their locations varied. Active JNK was found at the enhancer (primer A), the promoter (primer B), and downstream of the coding region (primer E) (Figure 5F). Phospho-MKK4 was localized to the enhancer, promoter, and downstream of the coding region (primer E) and MSN was localized to the promoter (primer B) (Figures 5H and 5J). Strikingly, like ATAC upon osmotic stress, occupancy of each of these kinases was increased in the coding region (primer D), the site of Jra binding (Figures 5G, 5I, and 5K). This was most significant for Active JNK, which bound strongly to the primer D region upon osmotic stress (note the difference in scale between Figures 5F and 5G), and for MSN, which relocalized from the promoter to the coding region (primer D) (Figures 5J and 5K).

The ChIP results from the knockdown cell lines indicate a dynamic interplay between ATAC and the upstream kinases. For example, in the absence of osmotic stress, H4K16 acetylation at the promoter (primer B) was independent of MSN (Figure 5D); however, upon osmotic stress, MSN suppressed H4K16 acetylation at the promoter but was required for maximum acetylation in the coding region (primer D) (Figure 5E). In the absence of osmotic stress, the binding of Active JNK to the enhancer, promoter, and downstream of the coding region required ATAC but was suppressed by MSN (Figure 5F). By contrast, under osmotic stress, the strong binding of Active JNK to the coding region (primer D) required both ATAC and MSN (Figure 5G). In the absence of osmotic stress, binding of phospho-MKK4 to the enhancer was suppressed by ATAC and MSN (Figure 5H) but upon osmotic stress, binding to the promoter required MSN and CG10238 specifically (Figure 5I).

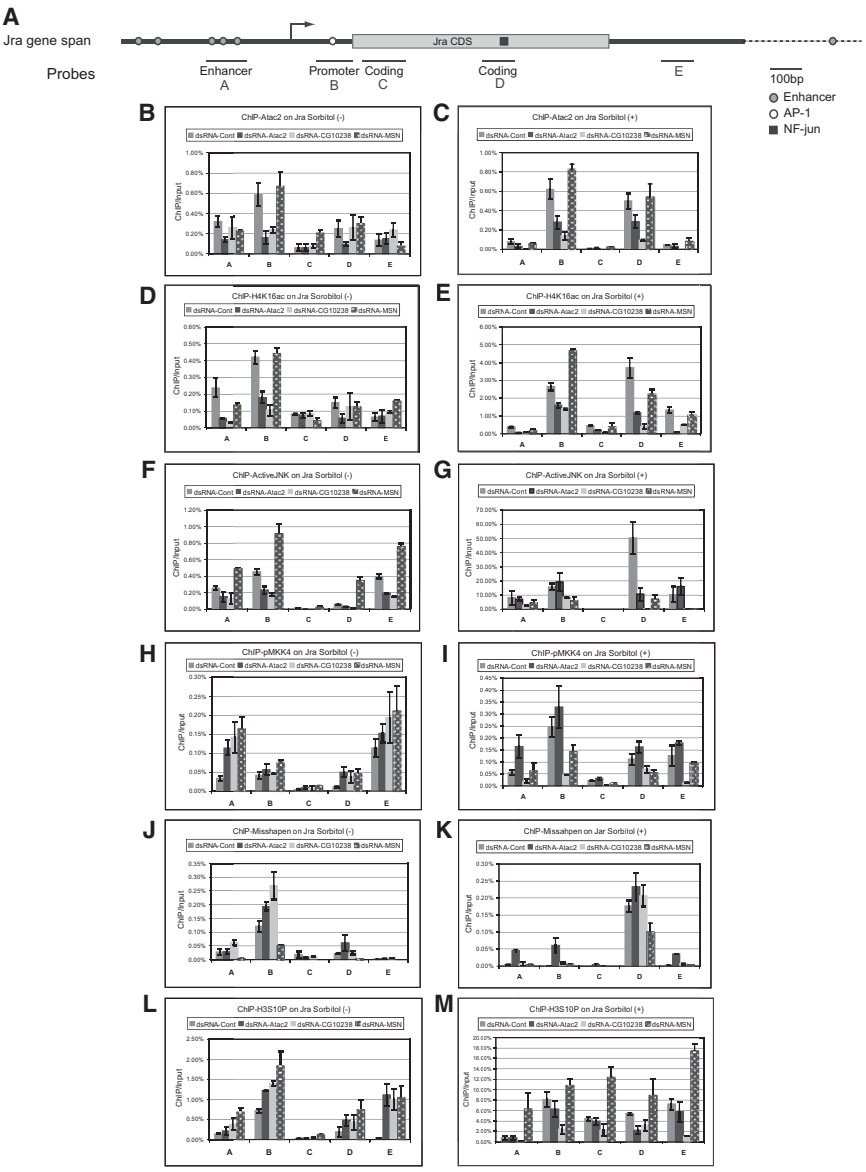

Figure 5. Occupancy of ATAC, H4K16 Acetylation, MAPKs, and H3S10P on the *Jra* Gene with and without Osmotic Stress

(A) Schematic representation of the *Jra* gene indicating the position of different probes tested (A–E on x axis for B–M). The gray box indicates the coding sequence (CDS), the gray circles indicate the enhancer, the white circle indicates predicted AP-1 sites, and the black square indicates the NF-jun-like sequence.

(B–M) ChIP assays were performed with antibodies against Atac2, H4K16ac, Active JNK, phospho-MKK4 (S257T261) (pMKK4), MSN, and phospho-H3S10 (H3S10P) from ATAC and MSN knockdown S2 cells (as in Figure 4D) without sorbitol stimulation (B, D, F, H, J, and L) (Figures 6B, 6D, 6F, 6H, and 6J) or with sorbitol stimulation (C, E, G, I, K, M) (Figures 6C, 6E, 6G, 6I, and 6K) on the probed region of the *Jra* gene as indicated in (A), and input chromatin was measured by qRT-PCR and normalized to input. The ratios of measured quantities are represented (see Figures S5A and S6). The average of three independent experiments is graphed. Error bars represent standard deviation.

See also Figures S2, S5, and S6.

Finally, binding of MSN to the promoter is suppressed by ATAC in the absence of osmotic stress (Figure 5J); however, when it moves to the coding region where Jra is bound (primer D), upon osmotic stress its binding is independent of ATAC (Figure 5K).

A previous study linked the acetylation of H4K16 with H3S10 phosphorylation in the activation of the *FOSL1* gene (Zippo et al., 2009). At this gene, H3S10 phosphorylation was reported to recruit MOF-dependent H4K16 acetylation, which then recruited the elongation factor P-TEFb to release paused polymerase (Zippo et al., 2009). As ATAC is also an H4K16 acetyltransferase, we tested for a relationship between H3S10 phosphorylation and H4K16 acetylation, ATAC, or MSN at *Jra*. H3S10P was enriched in the enhancer and promoter regions (primer B) in the absence of osmotic stress (Figure 5L). H3S10 phosphorylation levels were suppressed by ATAC and MSN at the promoter and strongly suppressed downstream of the coding region (Figure 5L). Osmotic stress substantially increased H3S10 phosphorylation levels across the *Jra* gene except for the upstream enhancer (note the different scales in Figures 5L and 5M). Induction of H3S10 phosphorylation at the promoter, the coding region (primer D), and downstream of the coding region depended on ATAC (especially CG10238); however, MSN suppressed H3S10 phosphorylation across the gene (Figure 5M). These results suggest that the relationship between H3S10 phosphorylation and H4K16 acetylation by ATAC at *Jra* differs from what was observed with H3S10 phosphorylation and H4K16 acetylation by MOF at the *FOSL1* gene (Zippo et al., 2009). Acetylation of H4K16 at the enhancer of FOSL1 by MOF required H3S10 phosphorylation; however, ATAC is required for H3S10 phosphorylation in the presence of osmotic stress. Moreover, ATAC-dependent H4K16 acetylation at the *Jra* enhancer in the absence of osmotic stress (Figure 5D) occurred independently of significant H3S10 phosphorylation (Figure 5L).

ATAC Acetylates Nucleosomes and Coordinates the JNK Upstream Kinases with Jra on *chickadee*

The most striking aspect of our ChIP analysis of the *Jra* gene is the movement upon osmotic stress of ATAC and MAPKs to the coding region (primer D), which contains an NF-jun binding sequence and is occupied by the Jra transcription factor. This

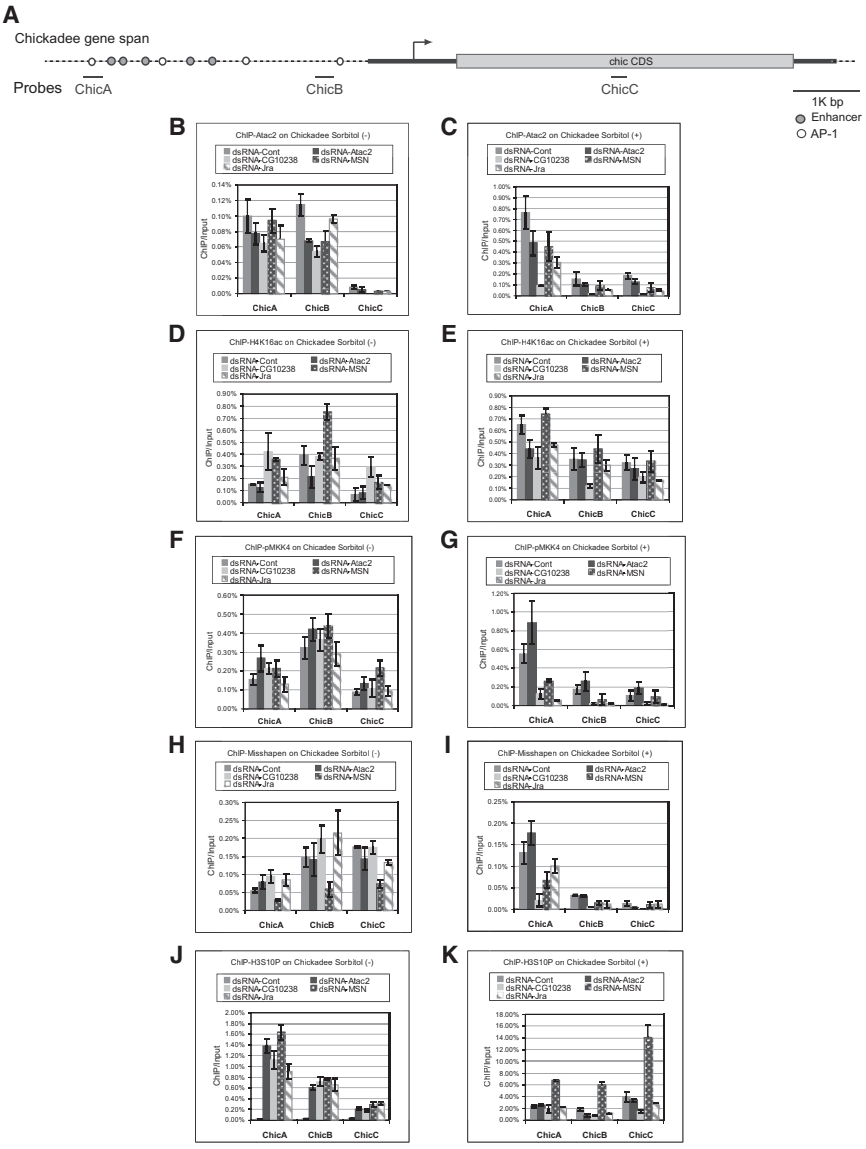

Figure 6. Occupancy of ATAC, H4K16 Acetylation, MAPKs, and H3S10P on the *chickadee* Gene with and without Osmotic Stress

(A) Schematic representation of the *chickadee* gene including 7 kb upstream of the transcription start site indicating the position of different probes on the gene (ChicA-C on x axis for B–K). The gray box indicates the coding sequence (CDS), the gray circles indicate the enhancer, and the white circles indicate predicted AP-1 sites.

(B–K) ChIP assays were performed with antibodies against Atac2, H4K16ac, pMKK4 (S257T261), MSN, and phospho-H3S10 (H3S10P) from ATAC and MSN knockdown S2 cells with or without sorbitol stimulation (as in Figure 4D) on the probed region of the *chickadee* gene and upstream region as indicated in (A), and input chromatin was measured by qRT-PCR and normalized to input (see Figure S7A). The ratios of the measured quantities are represented. The average of three independent experiments is graphed. Error bars represent standard deviation.

See also Figures S2, S5, S6, and S7.

raised the question as to whether ATAC and MAPKs move to this location because Jra is bound there or because they need to associate with the coding region. Thus, we performed a ChIP assay on another JNK target gene, *chickadee*. Chickadee does not have an apparent NF-jun binding site in the coding region. It does, however, have several AP-1-like sequences upstream of the promoter and at a far-upstream enhancer (Figure 6A). We analyzed 7 kb upstream of the *chickadee* gene and found five AP-1-like sequences. We probed a region containing an AP-1-like site, which was also near two CCAAT motifs that are 6.4 kb upstream from the coding sequence (ChicA primer). We also probed adjacent to the AP-1-like site 2 kb upstream from the coding sequence close to the predicted promoter (ChicB primer) and the middle of the coding region (ChicC primer) (Figure 6A). ChIP analysis revealed that Jra was localized at the ChicA and ChicB regions, suggesting Jra binds AP-1 sites on *chickadee* (Figure S7A). Jra occupancy was reduced in CG10238 and MSN knockdown cells but not in Atac2 knockdown cells (Figure S7A). These two regions were co-occupied by ATAC and H4K16 acetylation (Figures 6B and 6D). The presence of Atac2 and H4K16 acetylation at these regions was not affected by the knockdown of Jra, suggesting ATAC does not require Jra to bind the *chickadee* gene in the absence of osmotic stress. Interestingly, in the presence of osmotic stress, ATAC occupancy and H4K16 acetylation were increased at the ChicA region, and this increased occupancy was reduced in Jra knockdown cells (Figures 6C and 6E). Phospho-MKK4 and MSN also occupied the ChicA and ChicB regions, and these kinases were also found in the open reading frame (ChicC) in the absence of osmotic stress (Figures 6F and 6H). In contrast to what was seen at the *Jra* gene, on *chickadee* the kinases move to the upstream ChicA region upon osmotic stress and their occupancy is largely (MKK4) or slightly (MSN) dependent on Jra (Figures 6G and 6I). Occupancy of ChicA by the kinases under these conditions is slightly suppressed by Atac2 but completely dependent on CG10238. Indeed, CG10238 was crucial for the occupancy of ATAC, MKK4, and MSN on the far-upstream ChicA region under conditions of osmotic stress (Figures 6C, 6G, and 6I). At the *Jra* gene, occupancy of the primer D region containing the NF-Jun binding site by ATAC, Active JNK, and phospho-MKK4 upon osmotic stress was dependent on CG10238. As seen on *Jra*, H3S10P on *chickadee* was suppressed by ATAC and MSN in the absence of osmotic stress and, although H3S10P increased upon osmotic stress, these levels were suppressed by MSN specifically (Figures 6J and 6K).

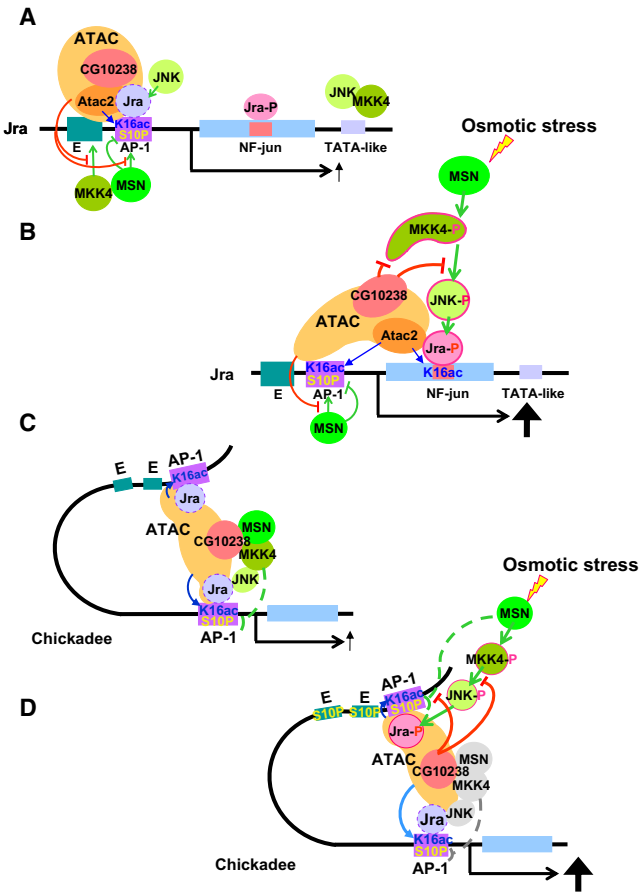

Figure 7. Models Summarizing ATAC Functions and the Molecular Events Occurring on *Jra* and *chickadee* as Revealed by the ChIP Data

Summaries of ChIP data on the *Jra* gene without and with osmotic stress are shown in (A) and (B), respectively. Summaries of ChIP data on the *chickadee* gene without and with osmotic stress are shown in (C) and (D), respectively.

(A) In the absence of osmotic stress, ATAC occupies and acetylates H4K16 (K16ac) at the enhancer (E) and promoter regions, containing AP-1 sites (AP-1), of the *Jra* gene and is required for basal levels of *Jra* transcription (small arrow). ATAC blocks the recruitment of MKK4 to the enhancer and MSN to the promoter while inhibiting the activation of JNK. The phosphorylation of H3S10 (S10P) on the promoter region is suppressed by MSN.

(B) When cells are exposed to osmotic stress, the stress-activated kinases in the JNK cascade are recruited to the Jra binding motif (NF-jun) on the *Jra* gene by ATAC, especially dependent on CG10238. In addition to interacting with the promoter region, ATAC also interacts with the NF-jun site by interaction with Jra and further acetylates H4K16 at this site. ATAC continues to limit the extent of JNK activation. Phosphorylation of H3S10 is increased across the *Jra* gene by osmotic stress but is still suppressed by MSN. *Jra* transcription is rapidly and transiently induced (large arrow).

(C) The *chickadee* gene does not have an apparent NF-jun site. In the absence of osmotic stress, Jra, ATAC, and acetyl-H4K16 are found at two AP-1 sites, which are 2 and 7 kb upstream from the coding sequence. Upstream kinases occupy these sites and the downstream coding region.

(D) In the presence of osmotic stress, ATAC preferentially relocalizes to the far-upstream AP-1 site and recruits Jra to this location. Phospho-MKK4 (MKK4-P) and MSN are also relocalized to this far-upstream AP-1 site in a CG10238- and Jra-dependent manner. The CG10238 subunit of ATAC is required for ATAC, Jra, MKK4-P, and MSN relocalization to the far-upstream enhancer. Transcription of *chickadee* is activated (large arrow) whereas the levels of phosphorylated H3S10 are suppressed by MSN across the *chickadee* gene.

See also Figure S7.

The models presented in Figure 7 summarize the molecular events occurring on *Jra* and *chickadee* as revealed by the ChIP data. Although differing in details having to do with the architecture of each gene, comparison of the expression and ChIP data from *Jra* and *chickadee* reveals strikingly common features about the role of ATAC at these genes. First, in the absence of osmotic stress, ATAC is required for the basal expression of these genes, which is most highly dependent on the Atac2 acetyltransferase subunit. Second, upon osmotic stress, ATAC suppresses induced transcription levels of these genes, which is most highly dependent on the CG10238 subunit. Third, upon osmotic stress, ATAC and the MAPKs move to the region of the gene where Jra is bound. And fourth, the relocalization of ATAC and MAPKs is dependent on CG10238, the MAP kinase upstream kinase binding inhibitory protein. Thus, ATAC coordinates the occupancy of Jra and upstream kinases while it controls the levels of JNK activation and target gene induction.

DISCUSSION

ATAC shares four subunits with the SAGA transcription coactivator complex and was anticipated to function as a coactivator. However, preliminary studies indicated that ATAC did not interact with the activation domains of VP16 or p53 under conditions in which SAGA bound (Kusch et al., 2003). Prompted by the identification of peptides from the Jra (*Drosophila* c-Jun) transcription factor in ATAC affinity purifications, we demonstrated that Jra coimmunoprecipitates with ATAC subunits. We further demonstrate that ATAC is localized to Jra target genes (*Jra* and *chickadee*) and is required for H4K16 acetylation at the *Jra* and *chickadee* enhancer and promoter. ATAC was required for basal levels of expression of these genes, which depended strongly on the Atac2 acetyltransferase subunit. Thus, to our knowledge, this is the first report to demonstrate that ATAC functions as a transcription cofactor.

Our pursuit of the functions of the CG10238 subunit of ATAC and the potential role of its MoaE domain led us to discover that ATAC is intimately integrated into MAP kinase signaling and target gene expression. CG10238 was found to inhibit JNK activation by osmotic stress, an activity mediated through the MoaE domain. Thus, structural features of this protein that are utilized for molybdopterin synthesis have been conscripted in ATAC to function in the regulation of MAP kinase signaling. The MSN kinase is the most likely direct target of CG10238, as it coimmunoprecipitates with ATAC subunits. However, we cannot rule out potential interactions with other kinases; for example, peptides from MKK4 have been found in ATAC purifications (Figure 1). Under conditions of osmotic stress, ATAC suppresses the level of target gene expression in a manner strongly dependent on CG10238. We believe this is due to inhibition of JNK activation rather than a direct negative effect of ATAC on transcription. In fact, ATAC may still function as a positive cofactor for induced Jra expression, as the levels of H3S10P on the gene, considered a positive mark for transcription

(Zippo et al., 2009), are dependent on ATAC (Figure 5M). In a manner strongly dependent on CG10238, ATAC plays a striking role in the binding of MAPKs to the *Jra* and *chickadee* genes. Upon osmotic stress, ATAC was required for the recruitment of the JNK, MKK4, and MSN kinases to the site of Jra binding. The only exception was the binding of MSN to the *Jra* gene (Figure 5K). However, MSN required CG10238 for binding *chickadee* under inducing conditions (Figure 6I). The crucial role of CG10238 in both the recruitment of the kinases and the inhibition of signaling is most consistent with a model by which ATAC inhibits JNK activation at the downstream target genes. The fact that ATAC and the MAPKs all move to the site of Jra binding suggests that a localized signaling network is organized at the site occupied by the downstream transcription factor.

Our data indicate that a positive cofactor of JNK target gene transcription, ATAC, also serves to negatively feed back for inhibition of the JNK signaling pathway. Why would a downstream activator also repress upstream signaling? The JNK pathway and c-Jun have been shown to suppress p53-dependent apoptosis and cellular senescence (Alexaki et al., 2008; Butterfield et al., 1997; Das et al., 2007; Fan et al., 2010; Ham et al., 2000; Takekawa and Saito, 1998; Yang et al., 1997). Moreover, c-Jun has been shown to repress transcription of the p53 gene and hence its downstream targets (Schreiber et al., 1999). Thus, a delicate balance of JNK signaling and p53 expression controls cell growth, proliferation, and apoptosis. If ATAC suppression of JNK is involved in this process, we might expect loss of ATAC to result in decreased expression of p53 due to increased JNK activity (Schreiber et al., 1999). Indeed, whereas knockdown of Jra increased p53 expression in S2 cells, knockdown of ATAC subunits resulted in a decrease in p53 expression consistent with ATAC suppression of JNK activation (Figure S7B).

Our results reveal a mechanism for governing the transcriptional response to signaling pathways. By serving as both a downstream transcriptional cofactor and as an inhibitor of upstream signaling, ATAC serves as a master regulator which administers the appropriate level of response to the inducing signals.

EXPERIMENTAL PROCEDURES

Cell Lines, Extract Preparation, and Complex Purification

The nuclear extracts from S2 cell lines were generated as described in Extended Experimental Procedures and were used for FLAG affinity purification as previously described (Suganuma et al., 2008).

Chromatin Immunoprecipitation Assay

The crosslinked S2 cell pellets were washed, resuspended, and sonicated, and the DNA was immunoprecipitated with antibodies using Dynabeads (Invitrogen). The bound DNA and input DNA were incubated with RNaseA and the crosslinking was reversed. The ethanol-precipitated DNA pellets were resuspended and then were analyzed by quantitative real-time RT-PCR. Antibodies, buffer content, and primers for ChIP-qRT-PCR are described in the Extended Experimental Procedures.

Osmotic Stress Response in dsRNAi Knockdown S2 Cells and siRNA Knockdown 293T Cells

The dsRNAi was transfected in S2 cells. The siRNA was transfected in 293T cells as described in the Extended Experimental Procedures. The cells were incubated with 500 mM sorbitol for 12 min before harvest.

Multidimensional Protein Identification Technology Analysis

MudPIT analysis was performed as described in the Extended Experimental Procedures.

SUPPLEMENTAL INFORMATION

Supplemental Information includes Extended Experimental Procedures and seven figures and can be found with this article online at doi:10.1016/j.cell.2010.07.045.

ACKNOWLEDGMENTS

We thank the Workman Lab members, Bjoern Gaertner in the Zeitlinger Lab, and Hidehisa Takahashi in the Conaway Lab for advice and support during this project. This research was supported by the Stowers Institute for Medical Research.

Received: December 30, 2009
Revised: May 14, 2010
Accepted: July 1, 2010
Published: September 2, 2010

REFERENCES

Alepuz, P.M., Jovanovic, A., Reiser, V., and Ammerer, G. (2001). Stress-induced MAP kinase Hog1 is part of transcription activation complexes. Mol. Cell *7*, 767–777.

Alepuz, P.M., de Nadal, E., Zapater, M., Ammerer, G., and Posas, F. (2003). Osmostress-induced transcription by Hot1 depends on a Hog1-mediated recruitment of the RNA Pol II. EMBO J. *22*, 2433–2442.

Alexaki, V.I., Javelaud, D., and Mauviel, A. (2008). JNK supports survival in melanoma cells by controlling cell cycle arrest and apoptosis. Pigment Cell Melanoma Res *21*, 429–438.

Altschul, S.F., Madden, T.L., Schaffer, A.A., Zhang, J., Zhang, Z., Miller, W., and Lipman, D.J. (1997). Gapped BLAST and PSI-BLAST: a new generation of protein database search programs. Nucleic Acids Res. *25*, 3389–3402.

Angel, P., and Karin, M. (1991). The role of Jun, Fos and the AP-1 complex in cell-proliferation and transformation. Biochim. Biophys. Acta *1072*, 129–157.

Angel, P., Hattori, K., Smeal, T., and Karin, M. (1988). The jun proto-oncogene is positively autoregulated by its product, Jun/AP-1. Cell *55*, 875–885.

Butterfield, L., Storey, B., Maas, L., and Heasley, L.E. (1997). c-Jun NH_2-terminal kinase regulation of the apoptotic response of small cell lung cancer cells to ultraviolet radiation. J. Biol. Chem. *272*, 10110–10116.

Ciurciu, A., Komonyi, O., Pankotai, T., and Boros, I.M. (2006). The *Drosophila* histone acetyltransferase Gcn5 and transcriptional adaptor Ada2a are involved in nucleosomal histone H4 acetylation. Mol. Cell. Biol. *26*, 9413–9423.

Das, M., Jiang, F., Sluss, H.K., Zhang, C., Shokat, K.M., Flavell, R.A., and Davis, R.J. (2007). Suppression of p53-dependent senescence by the JNK signal transduction pathway. Proc. Natl. Acad. Sci. USA *104*, 15759–15764.

de Nadal, E., and Posas, F. (2010). Multilayered control of gene expression by stress-activated protein kinases. EMBO J. *29*, 4–13.

de Nadal, E., Alepuz, P.M., and Posas, F. (2002). Dealing with osmostress through MAP kinase activation. EMBO Rep. *3*, 735–740.

de Nadal, E., Zapater, M., Alepuz, P.M., Sumoy, L., Mas, G., and Posas, F. (2004). The MAPK Hog1 recruits Rpd3 histone deacetylase to activate osmoresponsive genes. Nature *427*, 370–374.

Devary, Y., Gottlieb, R.A., Lau, L.F., and Karin, M. (1991). Rapid and preferential activation of the c-jun gene during the mammalian UV response. Mol. Cell. Biol. *11*, 2804–2811.

Dioum, E.M., Wauson, E.M., and Cobb, M.H. (2009). MAP-ping unconventional protein-DNA interactions. Cell *139*, 462–463.

Edmunds, J.W., and Mahadevan, L.C. (2004). MAP kinases as structural adaptors and enzymatic activators in transcription complexes. J. Cell Sci. *117*, 3715–3723.

Fan, Y., Lee, T.V., Xu, D., Chen, Z., Lamblin, A.F., Steller, H., and Bergmann, A. (2010). Dual roles of *Drosophila* p53 in cell death and cell differentiation. Cell Death Differ. *17*, 912–921.

Fukuyama, K., Yoshida, M., Yamashita, A., Deyama, T., Baba, M., Suzuki, A., Mohri, H., Ikezawa, Z., Nakajima, H., Hirai, S., et al. (2000). MAPK upstream kinase (MUK)-binding inhibitory protein, a negative regulator of MUK/dual leucine zipper-bearing kinase/leucine zipper protein kinase. J. Biol. Chem. *275*, 21247–21254.

Guelman, S., Suganuma, T., Florens, L., Swanson, S.K., Kiesecker, C.L., Kusch, T., Anderson, S., Yates, J.R., III, Washburn, M.P., Abmayr, S.M., et al. (2006). Host cell factor and an uncharacterized SANT domain protein are stable components of ATAC, a novel dAda2A/dGcn5-containing histone acetyltransferase complex in *Drosophila*. Mol. Cell. Biol. *26*, 871–882.

Ham, J., Eilers, A., Whitfield, J., Neame, S.J., and Shah, B. (2000). c-Jun and the transcriptional control of neuronal apoptosis. Biochem. Pharmacol. *60*, 1015–1021.

Hu, S., Xie, Z., Onishi, A., Yu, X., Jiang, L., Lin, J., Rho, H.S., Woodard, C., Wang, H., Jeong, J.S., et al. (2009). Profiling the human protein-DNA interactome reveals ERK2 as a transcriptional repressor of interferon signaling. Cell *139*, 610–622.

Iyer, L.M., Burroughs, A.M., and Aravind, L. (2006). The prokaryotic antecedents of the ubiquitin-signaling system and the early evolution of ubiquitin-like β-grasp domains. Genome Biol. *7*, R60.

Jasper, H., Benes, V., Schwager, C., Sauer, S., Clauder-Munster, S., Ansorge, W., and Bohmann, D. (2001). The genomic response of the *Drosophila* embryo to JNK signaling. Dev. Cell *1*, 579–586.

Kayali, A.G., Austin, D.A., and Webster, N.J. (2000). Stimulation of MAPK cascades by insulin and osmotic shock: lack of an involvement of p38 mitogen-activated protein kinase in glucose transport in 3T3-L1 adipocytes. Diabetes *49*, 1783–1793.

Kimura, A., Matsubara, K., and Horikoshi, M. (2005). A decade of histone acetylation: marking eukaryotic chromosomes with specific codes. J. Biochem. *138*, 647–662.

Kusch, T., Guelman, S., Abmayr, S.M., and Workman, J.L. (2003). Two *Drosophila* Ada2 homologues function in different multiprotein complexes. Mol. Cell. Biol. *23*, 3305–3319.

Kyriakis, J.M., and Avruch, J. (2001). Mammalian mitogen-activated protein kinase signal transduction pathways activated by stress and inflammation. Physiol. Rev. *81*, 807–869.

Lawrence, M.C., Shao, C., McGlynn, K., Naziruddin, B., Levy, M.F., and Cobb, M.H. (2009). Multiple chromatin-bound protein kinases assemble factors that regulate insulin gene transcription. Proc Natl Acad Sci USA *106*, 22181–22186.

Lee, K.K., and Workman, J.L. (2007). Histone acetyltransferase complexes: one size doesn't fit all. Nat. Rev. Mol. Cell Biol. *8*, 284–295.

Leimkuhler, S., Freuer, A., Araujo, J.A., Rajagopalan, K.V., and Mendel, R.R. (2003). Mechanistic studies of human molybdopterin synthase reaction and characterization of mutants identified in group B patients of molybdenum cofactor deficiency. J. Biol. Chem. *278*, 26127–26134.

Mas, G., de Nadal, E., Dechant, R., Rodriguez de la Concepcion, M.L., Logie, C., Jimeno-Gonzalez, S., Chavez, S., Ammerer, G., and Posas, F. (2009). Recruitment of a chromatin remodelling complex by the Hog1 MAP kinase to stress genes. EMBO J. *28*, 326–336.

Morrison, D.K., Murakami, M.S., and Cleghon, V. (2000). Protein kinases and phosphatases in the *Drosophila* genome. J. Cell Biol. *150*, F57–F62.

Pokholok, D.K., Zeitlinger, J., Hannett, N.M., Reynolds, D.B., and Young, R.A. (2006). Activated signal transduction kinases frequently occupy target genes. Science *313*, 533–536.

Proft, M., Mas, G., de Nadal, E., Vendrell, A., Noriega, N., Struhl, K., and Posas, F. (2006). The stress-activated Hog1 kinase is a selective transcriptional elongation factor for genes responding to osmotic stress. Mol. Cell *23*, 241–250.

Rozek, D., and Pfeifer, G.P. (1993). In vivo protein-DNA interactions at the c-jun promoter: preformed complexes mediate the UV response. Mol. Cell. Biol. *13*, 5490–5499.

Rozek, D., and Pfeifer, G.P. (1995). In vivo protein-DNA interactions at the c-jun promoter in quiescent and serum-stimulated fibroblasts. J. Cell. Biochem. *57*, 479–487.

Rudolph, M.J., Wuebbens, M.M., Rajagopalan, K.V., and Schindelin, H. (2001). Crystal structure of molybdopterin synthase and its evolutionary relationship to ubiquitin activation. Nat. Struct. Biol. *8*, 42–46.

Schreiber, M., Kolbus, A., Piu, F., Szabowski, A., Mohle-Steinlein, U., Tian, J., Karin, M., Angel, P., and Wagner, E.F. (1999). Control of cell cycle progression by c-Jun is p53 dependent. Genes Dev. *13*, 607–619.

Schwarz, G., and Mendel, R.R. (2006). Molybdenum cofactor biosynthesis and molybdenum enzymes. Annu. Rev. Plant Biol. *57*, 623–647.

Su, Y.C., Treisman, J.E., and Skolnik, E.Y. (1998). The *Drosophila* Ste20-related kinase misshapen is required for embryonic dorsal closure and acts through a JNK MAPK module on an evolutionarily conserved signaling pathway. Genes Dev. *12*, 2371–2380.

Suganuma, T., Gutierrez, J.L., Li, B., Florens, L., Swanson, S.K., Washburn, M.P., Abmayr, S.M., and Workman, J.L. (2008). ATAC is a double histone acetyltransferase complex that stimulates nucleosome sliding. Nat. Struct. Mol. Biol. *15*, 364–372.

Takekawa, M., and Saito, H. (1998). A family of stress-inducible GADD45-like proteins mediate activation of the stress-responsive MTK1/MEKK4 MAPKKK. Cell *95*, 521–530.

Thomson, S., Mahadevan, L.C., and Clayton, A.L. (1999). MAP kinase-mediated signalling to nucleosomes and immediate-early gene induction. Semin. Cell Dev. Biol. *10*, 205–214.

Treisman, J.E., Ito, N., and Rubin, G.M. (1997). misshapen encodes a protein kinase involved in cell shape control in *Drosophila*. Gene *186*, 119–125.

Wang, Y.L., Faiola, F., Xu, M., Pan, S., and Martinez, E. (2008). Human ATAC is a GCN5/PCAF-containing acetylase complex with a novel NC2-like histone fold module that interacts with the TATA-binding protein. J. Biol. Chem. *283*, 33808–33815.

Yang, D.D., Kuan, C.Y., Whitmarsh, A.J., Rincon, M., Zheng, T.S., Davis, R.J., Rakic, P., and Flavell, R.A. (1997). Absence of excitotoxicity-induced apoptosis in the hippocampus of mice lacking the Jnk3 gene. Nature *389*, 865–870.

Yang, S.H., Sharrocks, A.D., and Whitmarsh, A.J. (2003). Transcriptional regulation by the MAP kinase signaling cascades. Gene *320*, 3–21.

Zapater, M., Sohrmann, M., Peter, M., Posas, F., and de Nadal, E. (2007). Selective requirement for SAGA in Hog1-mediated gene expression depending on the severity of the external osmostress conditions. Mol. Cell. Biol. *27*, 3900–3910.

Zippo, A., Serafini, R., Rocchigiani, M., Pennacchini, S., Krepelova, A., and Oliviero, S. (2009). Histone crosstalk between H3S10ph and H4K16ac generates a histone code that mediates transcription elongation. Cell *138*, 1122–1136.